Smart Mater. Struct. **22** (2013) 014003 (11pp) doi:10.1088/0964-1726/22/1/014003

An IPMC-enabled bio-inspired bending/twisting fin for underwater applications

Viljar Palmre[1], Joel J Hubbard[2], Maxwell Fleming[2], David Pugal[1], Sungjun Kim[1], Kwang J Kim[1,3] and Kam K Leang[2]

[1] Active Materials and Processing Laboratory, Mechanical Engineering Department, University of Nevada—Reno, Reno, NV 89557-0312, USA
[2] Electroactive Systems and Controls Laboratory, Mechanical Engineering Department, University of Nevada—Reno, Reno, NV 89557-0312, USA
[3] Mechanical Engineering Department, University of Nevada—Las Vegas, Las Vegas, NV 89154-4027, USA

E-mail: kwang.kim@unlv.edu and kam@unr.edu

Received 11 July 2012, in final form 31 August 2012
Published 6 December 2012
Online at stacks.iop.org/SMS/22/014003

Abstract
This paper discusses the design, fabrication, and characterization of an ionic polymer–metal composite (IPMC) actuator-based bio-inspired active fin capable of bending and twisting motion. It is pointed out that IPMC strip actuators are used in the simple cantilever configuration to create simple bending (flapping-like) motion for propulsion in underwater autonomous systems. However, the resulting motion is a simple 1D bending and performance is rather limited. To enable more complex deformation, such as the flapping (pitch and heaving) motion of real pectoral and caudal fish fins, a new approach which involves molding or integrating IPMC actuators into a soft boot material to create an active control surface (called a 'fin') is presented. The fin can be used to realize complex deformation depending on the orientation and placement of the actuators. In contrast to previously created IPMCs with patterned electrodes for the same purpose, the proposed design avoids (1) the more expensive process of electroless plating platinum all throughout the surface of the actuator and (2) the need for specially patterning the electrodes. Therefore, standard shaped IPMC actuators such as those with rectangular dimensions with varying thicknesses can be used. One unique advantage of the proposed structural design is that custom shaped fins and control surfaces can be easily created without special materials processing. The molding process is cost effective and does not require functionalizing or 'activating' the boot material similar to creating IPMCs. For a prototype fin (90 mm wide × 60 mm long × 1.5 mm thick), the measured maximum tip displacement was approximately 44 mm and the twist angle of the fin exceeded 10°. Lift and drag measurements in water where the prototype fin with an airfoil profile was dragged through water at a velocity of 21 cm s^{-1} showed that the lift and drag forces can be affected by controlling the IPMCs embedded into the fin structure. These results suggest that such IPMC-enabled fin designs can be used for developing active propeller blades or control surfaces on underwater vehicles.

(Some figures may appear in colour only in the online journal)

1. Introduction

The ionic polymer–metal composite (IPMC) material, a type of electroactive polymer, is a unique active (smart) material with the advantages of being soft and flexible, requiring low driving voltage (<5 V), and having the ability to operate in aqueous environments. Recently, IPMCs have been considered for many applications, including underwater

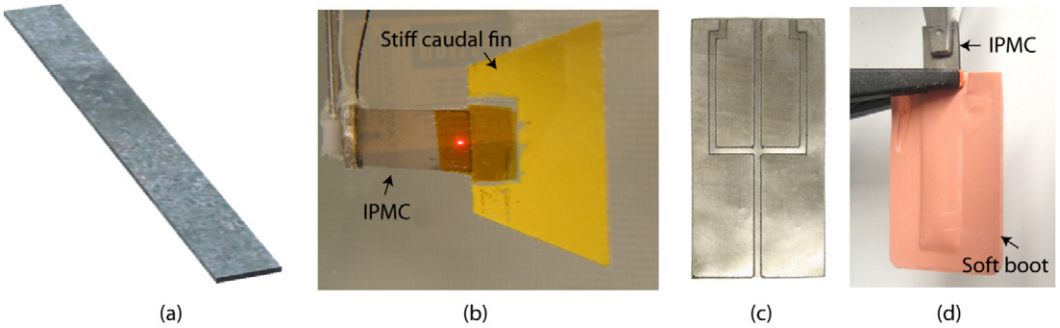

Figure 1. (a) Traditional IPMC strip (often used in cantilever configuration). (b) IPMC with passive stiff caudal fin. (c) Patterned electrodes on IPMC. (d) Proposed 'soft' boot with embedded IPMC.

robotics [1–5], various biomedical systems [6–9], and even for energy harvesting [10–12]. Much effort has focused on the use of IPMC actuators for propulsion and locomotion in underwater systems. Some unique advantages of IPMC-based propulsors include silent operation compared to traditional technologies such as pumps, jets, and propellers. Furthermore, the compactness and low power capabilities of IPMC actuators compared with traditional actuators such as DC motors make them more attractive for microautonomous systems. Traditionally, IPMCs are used in the simple cantilever configuration as illustrated in figure 1(a) to create bending (flapping-like) motion for propulsion in underwater autonomous systems, for example see [4, 13–15]. This approach is relatively straightforward and does not require special manufacturing to exploit the capabilities of the IPMC. However, the resulting motion is a simple 1D bending and propulsion performance is rather limited [16]. By integrating bio-inspired passive control surfaces (see figure 1(b)), such as stiff caudal fins, the propulsion behavior can be significantly enhanced [5, 16].

To enable more complex deformation, such as the flapping (pitch and heaving) motion of real pectoral and caudal fish fins, a bio-inspired approach has been taken where patterning of the IPMC electrodes has recently been explored to alter the bending behavior of traditional IPMCs (see figure 1(c)). It is pointed out that emerging underwater systems, such as autonomous ocean mapping and surveillance vehicles, can benefit from soft monolithic actuators and control surfaces capable of undergoing complex deformations. The patterning approach creates isolated electrodes on the IPMC membrane where, by applying different driving signals to different sectors of the IPMC, complex motion, specifically twisting, can be created [17, 18]. At the same time other regions can be patterned for sensing [19] fin deformation and responses to external stimulation. Contrast to approaches that combine flexible foils and interconnects between adjacent IPMC material, for example to create snake or worm-like robotic systems [20–23], the electrode patterning approach simplifies the manufacturing process to create monolithic IPMC structures which combine actuation and sensing capabilities into a compact structure. IPMCs with non-traditional shapes, such as disc-like structures [24], helical structures [25], and cylindrical shaped designs [26], have been investigated for applications that range from energy harvesting to active catheters in minimal invasive surgery.

Herein, a new approach is described which involves molding or integrating IPMC actuators into a soft boot material to create a bio-inspired control surface (called a 'fin') that can be used to realize complex deformation depending on the orientation and placement of the actuators. In contrast to previously created IPMCs with pattern electrodes for the same purpose [17, 18], the proposed design avoids (1) the more expensive process of electroless plating platinum all throughout the surface of the actuator and (2) the need for specially patterning the electrodes. Therefore, standard shaped IPMC actuators such as those with rectangular dimensions with different thicknesses can be used. One unique advantage of the proposed structural design is that custom shaped fins and control surfaces can be easily created without special materials processing. The molding process is relatively inexpensive and does not require functionalizing or 'activating' the boot material similar to creating IPMCs. Instead, the active IPMC material that provides actuation is inserted or molded into the soft boot structure. The result is a significant cost reduction by avoiding the need for electroless plating of platinum and electrode patterning or machining. Furthermore, the integrated IPMCs are protected from the surrounding environment for prolonged operation. Figure 1(d) illustrates the concept of the IPMC-enabled fin structure, where strips of IPMCs are incorporated into a relatively soft boot material to achieve both bending and twisting motion (figure 2(a)).

The main contribution of this work is the manufacturing, characterization, and feasibility demonstration of the newly created bio-inspired IPMC-controlled fin structure. The design of prototype IPMC-controlled fins is described in detail. Experimental results show that a fin undergoes bending (with tip displacement that exceeds 40 mm) and it can twist up to approximately 12°. A prototype design of a fin modeled after an NACA 0006 airfoil is tested in a drag tank. Experimental results demonstrate that the lift and drag forces can be affected by activating the IPMCs embedded within the fin structure at a speed of 21 cm s^{-1} in water. These results demonstrate the capabilities of the IPMC-enabled control surface for potential underwater applications, such as soft bio-inspired robotic platforms as illustrated in figure 2(b).

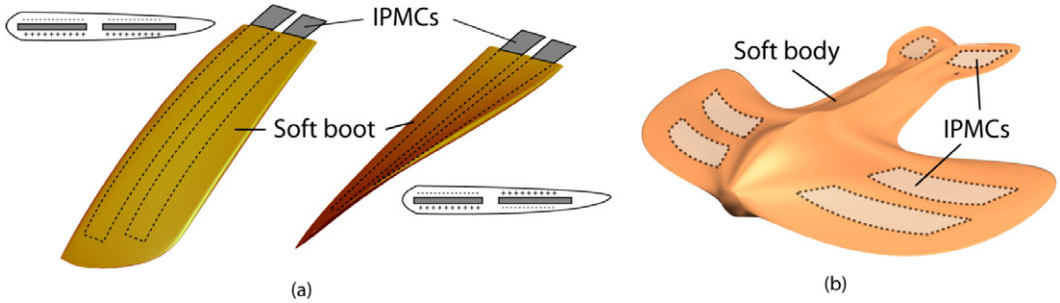

Figure 2. (a) IPMCs embedded into soft boot structure illustrating bending and twisting motion by selectively activating electrodes and (b) example soft bio-inspired robotic platform with embedded IPMC actuators for controlled deformation of control surfaces.

The remainder of this paper is outlined as follows. Section 2 describes the fabrication process for creating the IPMC actuators. Particularly, the discussion highlights the fabrication of thick IPMC membranes for creating actuators with higher output force than commercially available thin membranes. Next, the development of the soft boot structure is described in section 3. Experimental results and discussions are presented in section 4. Finally, concluding remarks are presented in section 5.

2. IPMC fabrication process

2.1. IPMC fabrication

A basic IPMC consists of an ion exchange polymer, for example Nafion (Dupont), sandwiched between two noble metallic electrodes such as platinum. The platinum electrode is often chemically deposited on the polymer's surface through a reduction process [27]. In the case of Nafion, the typical chemical structure consists of fluorocarbons, oxygen, sulfonate groups, and a mobile cation, which can be either hydrogen, sodium, or lithium. Commercially available Nafion membrane such as N115, N117, N1110 for fabricating IPMCs have nominal dry thicknesses of 127, 178, and 254 μm, respectively [5]. Methods to enhance the performance of IPMCs include boosting the capacitance of the composite [28, 29], where this is motivated by studies that correlate actuation and sensing performance with capacitance [28]. Enhancements in performance and blocking force have also been made by incorporating nanoparticulates into the polymer matrix [30, 31]. The nanocomposite-based IPMCs were observed to have higher water uptake and slower water loss, thus leading to larger bending displacement and blocking force. It was also found that by using a dispersing agent in the reduction process to form fine platinum polycrystals which subsequently lead to deeper penetration of the platinum layer, the blocking force was increased significantly [32]. More recent work to improve the output force involves increasing the thickness of the Nafion membrane [33]. Since a relatively thick Nafion membrane is not readily available, researchers have explored the solution casting process [33–36] and the hot pressing technique [37].

The output force enhancement for thicker IPMCs is evident by considering two IPMC strip actuators, both having the same length, width, but each have a different thicknesses, such as t and $2t$ (twice as thick). Assuming that for both actuators, the same tip displacement is required, then the required strain for the thick actuator is 2ϵ. As the stress tensor for linear beam with thickness of t, width b, and length L can be expressed [33]

$$\sigma_t = \frac{6F_tL}{bt^2}, \tag{1}$$

the ratio of the stresses is

$$\frac{\sigma_{2t}}{\sigma_t} \approx 2 = \frac{F_{2t}}{2^2F_t}, \tag{2}$$

hence $F_{2t} = 8F_t$. Therefore, a thicker IPMC will produce a larger blocking force. This result motivates the need to create thicker IPMC to produce larger output forces which can be exploited for deforming the boot structure.

In this work, a hot press approach was considered to create IPMCs with thicker profiles (see figure 3). Raw granules purchased from Ion Power Inc. (product name NR50) were used. First, the granules were cleaned in 0.3% H_2O_2 at 80 °C for 30 min followed by a rinse in 0.5 MH_2SO_4 at 80 °C for 30 min. Afterwards, the granules were dried in an oven, then pressed in a custom-designed mold at 400 °C at 5000 psi for 30 min. The activation process for the pellets (i.e., cation exchanging capability) is performed under hot aqueous NaOH or KOH. It is expected that the pellets are in an –SO2F-containing plastic initially and then converted to sulfonate groups (–SO3–Na+ or K+) after activation. Figure 3 illustrates the experimental procedure for manufacturing dimensionally scaleable polymer membrane(s).

The electroless plating process to create electrodes on the surface of the membrane begins with pre-treatment of the membrane. First, the surface of the membrane is either mechanically roughened or chemically etched [7] to either enhance the capacitance or to improve adhesion of the metal electrode to the surface. Then, organic and metallic impurities on the bare Nafion membrane are removed through a pre-treatment process by initially chemically cleaning the Nafion membrane in 3% hydrogen peroxide (H_2O_2). Next, the cleaned membrane is rinsed in 0.5 M sulfuric acid (H_2SO_4) at 80 °C to remove impurities. Afterwards, the pre-treated and cleaned Nafion membrane is immersed in an appropriate metal salt solution such as tetraammineplatinum

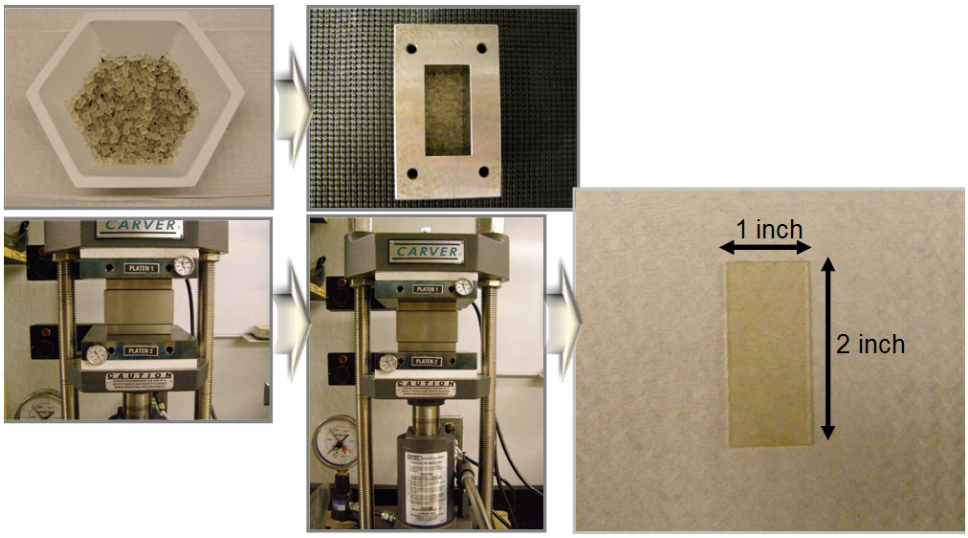

Figure 3. Experimental procedure for manufacturing of dimensionally scaleable polymer membrane(s), which begins with raw granules (top left photo) placed into a mold, followed by the hot pressing process.

(II) chloridemonohydrate ($[Pt(NH_3)_4] \cdot Cl_2xH_2O$) for 2 h, followed by several washings in de-ionized water. Platinum particles are metallized on the surface of the Nafion membrane by reducing the membrane in a sodium borohydride ($NaBH_4$) or lithium borohydride ($LiBH_4$) solution for 3 h. It is pointed out that the lithium-based IPMC actuators have shown adequate actuation performances with a bending strain up to 0.8% and a blocking force up to 14 g-force, which maybe suitable for use in small, underwater vehicles. Finally, the platinum plating process is repeated to achieve at least three layers of platinum on the surface of the Nafion membrane to enhance surface conductivity and overall performance. The platinum particulate layer is often buried 1–20 μm within the IPMC surface and is highly dispersed.

2.2. Surface enhancement via gold plating

Over time, performance degradation of the IPMC actuators can occur from the loss of mobile Li^+ cations as well as an increase in surface (electrode) resistance. Sometimes, the platinum electrode surface can develop cracks or voids from high levels of actuation or dehydration. Electroplating of gold to fill these voids and lower the surface resistance was considered to maintain as well as to improve performance. It is noted that newly fabricated IPMC had a surface resistance (measured by the two-point probe method) of 2.4 $\Omega/5$ cm before and 1.3 $\Omega/5$ cm after gold plating. For IPMCs that have been used extensively, the measured surface resistance increased to approximately 14 $\Omega/5$ cm. Shortly after gold plating, however, the resistance was reduced to approximately 1.4 $\Omega/5$ cm.

2.3. Output force performance

As an illustrative example of the generated force for thick IPMC sample, figure 4 shows the blocked force (truly the maximum force) measured by a load cell at the zero displacement condition (blocking force) for two different thicknesses of IPMCs (15 mm effective length and 5 mm width). Particularly, the force generated can be as high as 30 g-force. As can be seen, the thicker IPMC produced much larger blocking forces (1 mm versus 0.5 mm thick IPMC) and, also, the IPMCs with high-performance electrodes (Pd–Pt) show considerably higher blocking force compared to the conventional Pt IPMCs with respective thicknesses. At 3 V DC input, the blocking forces for 1 mm and 0.5 mm Pd–Pt IPMCs reach up to 20.1 and 6.1 g-force, whereas the forces for 1 mm and 0.5 mm Pt samples are up to 5 and 0.9 g-force. Moreover, at 4 V DC input, which is the upper limit of operating voltage, blocking forces as high as 31 and 10.5 g-force were recorded for the high-performance samples, and 10.8 and 2.9 g-force for the conventional Pt IPMC samples.

3. Soft IPMC fin structure design

Figure 5 illustrates the concept of embedding IPMC actuators into a soft boot (fin) structure to create control surfaces that can undergo complex bio-inspired deformation. As shown, standard IPMC strip actuators are incorporated into the overall structure. The number of actuators and their orientation can be tailored to achieve a desired performance. For the example shown, the three inserted IPMC actuators can be independently controlled to cause the fin to bend or twist. In particular, by driving the two outermost actuators with voltages of equal magnitude but opposite polarity, a twisting motion can be achieved. Equal polarity voltages leads to bending motion.

3.1. Prototype fabrication

Two molds were fabricated to create the fins for experiments. The first mold (FIN-A) is a simple rectangular shaped fin

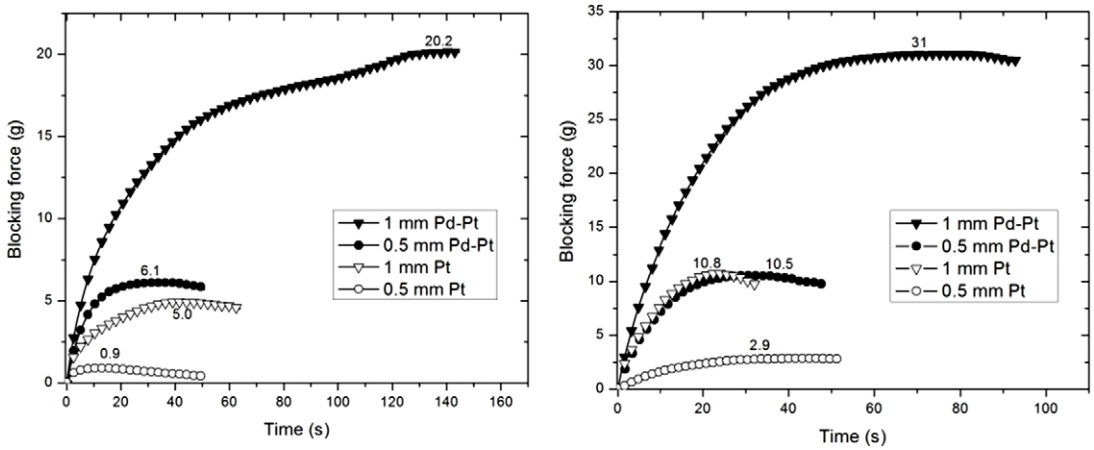

Figure 4. Blocking forces of the samples measured at 3 V and 4 V DC input, respectively.

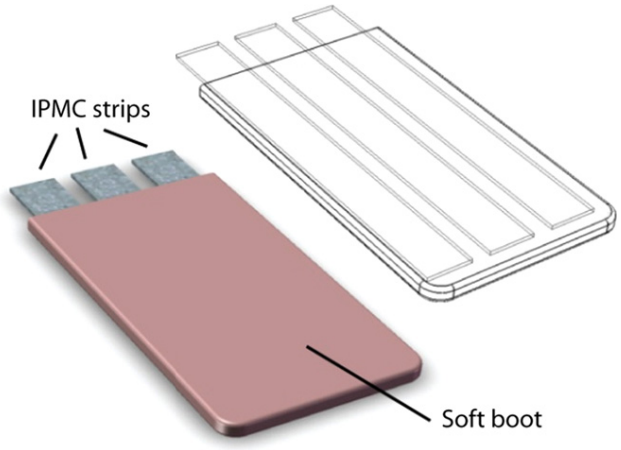

Figure 5. IPMC-enabled fin showing three embedded IPMC strip actuators.

(90 mm wide × 60 mm long × 1.5 mm thick), designed to house three IPMCs each with dimensions of 57 mm long × 11 mm wide × 0.5 mm thick. Three metal shims were used to create cavities inside of the mold to allow insertion of the IPMC actuators (see example in figure 5).

The second mold (FIN-B) is designed to mimic an airfoil (similar in shape to the blades used in the propulsion system described in [38]), modeled after the NACA 0006 profile. The dimensions of the second fin are approximately 60 mm wide × 80 mm long × 10 mm thick (at the leading edge). The mold for the NACA 0006 profile was machined into an aluminum block using a three-axis CNC milling machining.

Silicone casting rubber RTV 500 Resin by Hastings Plastics Company is used to fill the molds to make a flexible and high strength boot for the IPMCs. The modulus of the fin can be controlled to some degree through different mixing ratios between the base silicone and the catalyst. In this work, the silicone is mixed with a standard catalyst (Selfset 110–5)—one part of catalyst per 10 part of silicone, either by weight or volume. Both molds were sprayed with a mold release agent. Next, the silicone (mixed with the curing agent) was inserted into the bottom part of a mold. Shims were inserted into place to create cavities to house the IPMCs. Then the top mold was put in place and filled with the mixed silicone. The assembly was clamped together and allowed to cure for 24 h.

A similar boot structure, labeled FIN-C, (with similar profile to the NACA 0006 shape) provided by Dr Bandyopadhyay at Naval Undersea Warfare Center (NUWC), Rhode Island, was used for comparative mechanical studies (see figure 6). It is noted that the design is currently being considered for integration of IPMCs for controlling deformation, however, the fin is mechanically stiffer than the two silicone rubber designs proposed herein. Mechanical studies were performed on the fin as a means to assess the feasibility of the IPMCs for deforming fins that are of similar designs.

3.2. Mechanical properties

Mechanical testing was performed on FIN-C, the stiffer design, to determine the required force for deforming the fin structure. The experimental measurement system consists of a custom-designed IPMC control hardware (voltage amplifier, design described in [39]), laser displacement sensors, load cell, jack mechanism for displacing the fin, and computer and data acquisition system as shown in figure 6(a). The bending deflection and force were measured simultaneously. The stiffness of the fin, measured approximately 110 mm from the clamping point and 20 mm from the leading edge, shows a linear response, as indicated in figure 7(a). The average stiffness is approximately 1.9 gf mm^{-1}. The stiffness along the cord length at 110 mm distance from the clamped end is shown in figure 7(b), where the measured locations are indicated in figure 6(b). The non-uniform profile correlates with the cross-sectional shape of the fin, that is, the fin is thicker near its leading edge and thinner toward its trailing edge. The average stiffness along the cord length is approximately 1.87 gf mm^{-1}. Based on the bending stiffness of FIN-C, in order to achieve measurable deformation of the fin, IPMC strip actuators should provide output forces in the gram-force range.

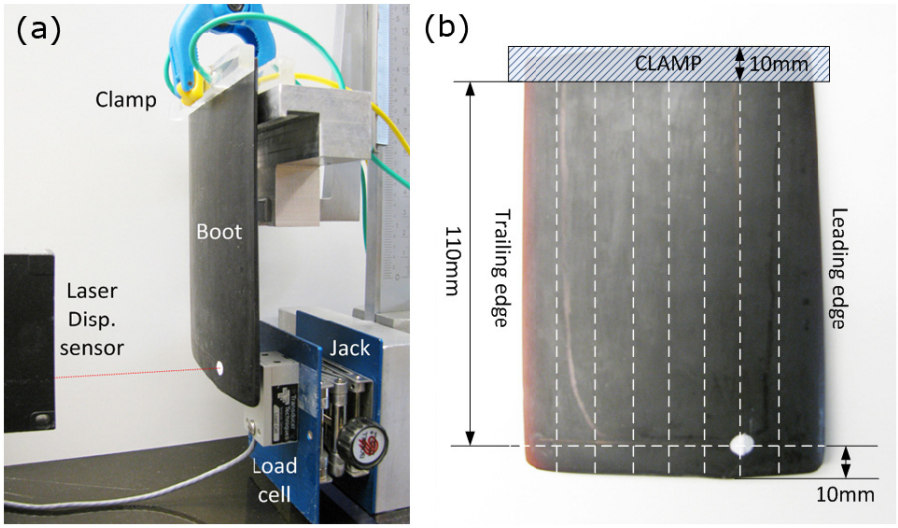

Figure 6. Mechanical testing on FIN-C: (a) experimental setup for measuring required force for deforming boot structure. (b) Location along boot where measurements were taken.

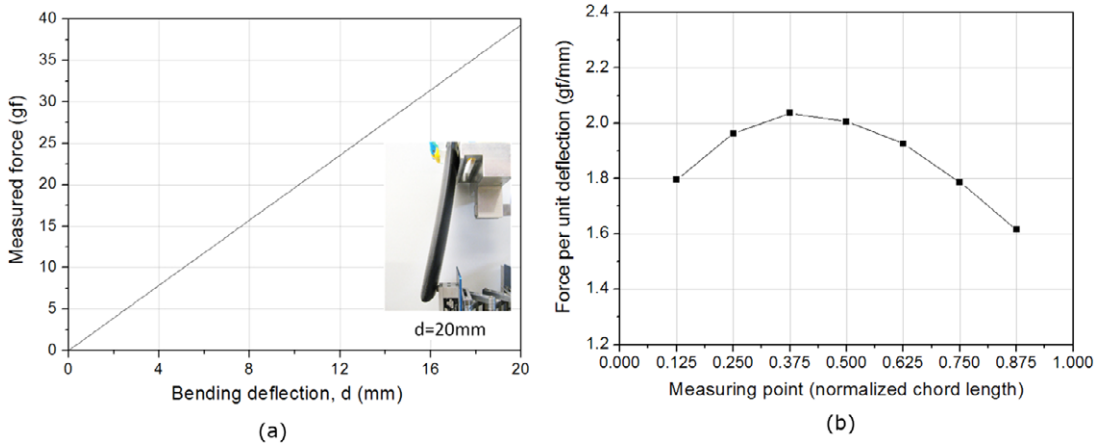

Figure 7. Force versus deflection curve measured (a) at one quarter of the chord length behind the leading edge of boot structure and (b) along the cord length.

The mechanical properties of the silicone rubber used to fabricate FIN-A and FIN-B were also measured using a three-point bending test. Samples of the material 3.1 mm thick and 26 mm wide were tested in an Instron machine. Flexure strain rates from 0.01 to 0.5 mm min^{-1} were applied. The first observation indicates that the Young's modulus of the material is bilinear (see figure 8). The Young's modulus for the second linear section ranges from 2.3 to 2.9 MPa, increasing with the increase of the strain rate. The stiffness of the silicone rubber is comparable to the stiffness of the IPMC material, suggesting that the embedded IPMC actuator will be capable of deforming the fin structure.

4. Performance characterization and discussion

Experiments were performed to characterize the response of the IPMC-based fin prototypes. Specifically, bending and twisting performance of FIN-A were measured. Drag tank experiments were performed on FIN-B to determine the effects on the drag and lift forces when the IPMCs were activated.

4.1. Bending and twisting performance

In order to properly constrain the IPMCs in a desired configuration a custom clamp is created. Its purpose is to not only provide adequate clamping force to hold the IPMCs in place but to maintain good electrical contact between the metallized surface of the IPMCs and the electrodes of the clamp. The FIN-A assembly (with three IPMC strip actuators) is clamped and placed near the surface of the water. For corrosion resistance, the electrodes were constructed out of stainless steel 304 and acrylic is chosen for the clamp itself as shown in figure 9. The boot-IPMC (FIN-A) and clamp fixture is suspended in a tank filled with tap water. The IPMCs were then actuated at 50 mHz with either a 4 V sine or square wave input signal.

First a bending test is conducted. To achieve maximum deflection, square wave input signals with the same phase are

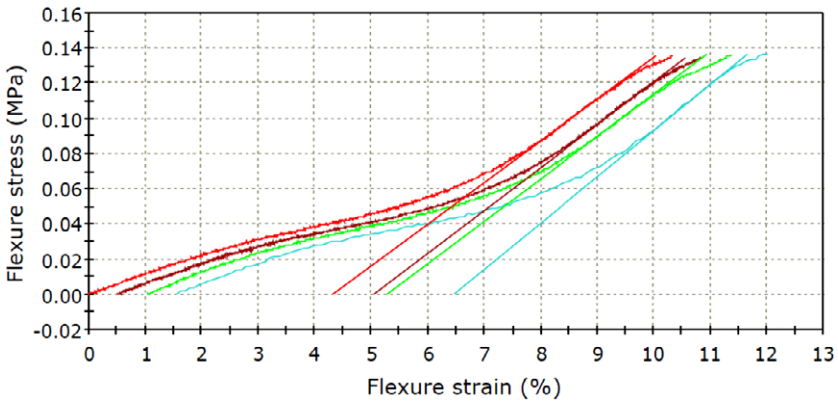

Figure 8. Flexure stress versus flexure strain for multiple applied strain rates (0.01, 0.05, 0.1, 0.5 mm min^{-1}) for silicone fin sample material. The lines indicate how the values of Young's modulus were calculated.

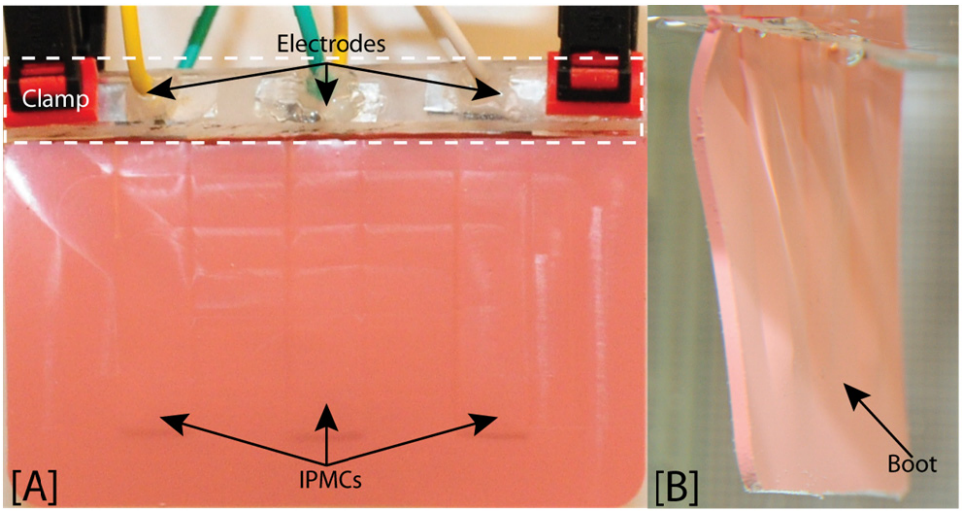

Figure 9. Experimental setup for FIN-A: (A) the clamp-boot-IPMC assembly and (B) the assembly ready for use.

applied to all three IPMCs in the boot. In figure 10, three consecutive images taken at intervals of 3.5 s illustrate the bending action relative to the input signal (vertical dash line corresponds to the time instant each image is acquired). A maximum tip deflection of 44 mm relative to the vertical is achieved. It is noted that the time response of the IPMC actuators for different DC input levels is illustrated in figure 4 for comparison.

Next a twisting motion is generated by phase shifting the same input signal by 180° between the two end IPMCs. The center IPMC is not actuated so as to not retard the movement of either adjacent actuators. A 50 mHz 4 V square wave signal was applied to actuate the boot-IPMC. In doing so the maximum twist angle was measured to be approximately 12° as shown in figure 11. The resulting twist angle is shown from two views in figure 11. Photographs show that due to the flexible boot material a complex shape is generated so that the angle varies both along the length and height of the boot.

The results from FIN-A driven by sine wave signals are compared to that of the square wave in table 1. The table shows that utilizing a square input signal generates larger deflections and twist angles compared to the sine wave input signal. This is expected; however, it is worth noting that using a square input signal does produce jarring movements. In addition, electrolysis becomes a much larger issue due to the prolonged time period at a susceptible voltage level.

Table 1. Results of bending and twisting performance of the FIN-A for sine and square wave input voltages.

	4 V amp. 50 mHz sine wave	4 V amp. 50 mHz square wave
Bending behavior	Tip deflection 36 mm	Tip deflection 43 mm
Twisting behavior	Maximum angle 10°	Maximum angle 12°

4.2. Characterization of drag and lift force

The effects of input voltage on the lift and drag forces on FIN-B, the design based on the NACA 0006 airfoil profile, were measured. A custom drag tank experiment was designed

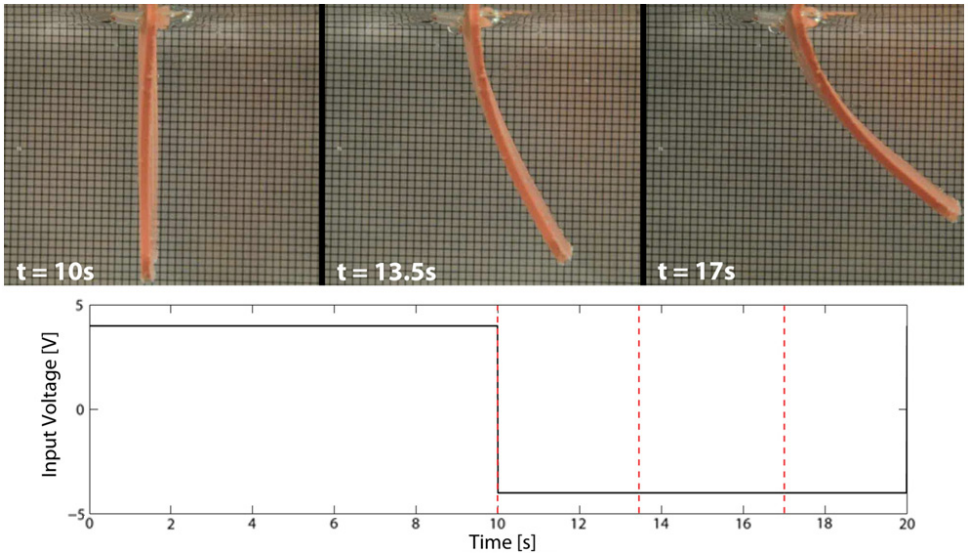

Figure 10. Consecutive images of boot-IPMC (FIN-A) assembly bending due to a 4 V amplitude 50 mHz square wave input signal. The times corresponding to the images are indicated by the red dotted lines in the plot below.

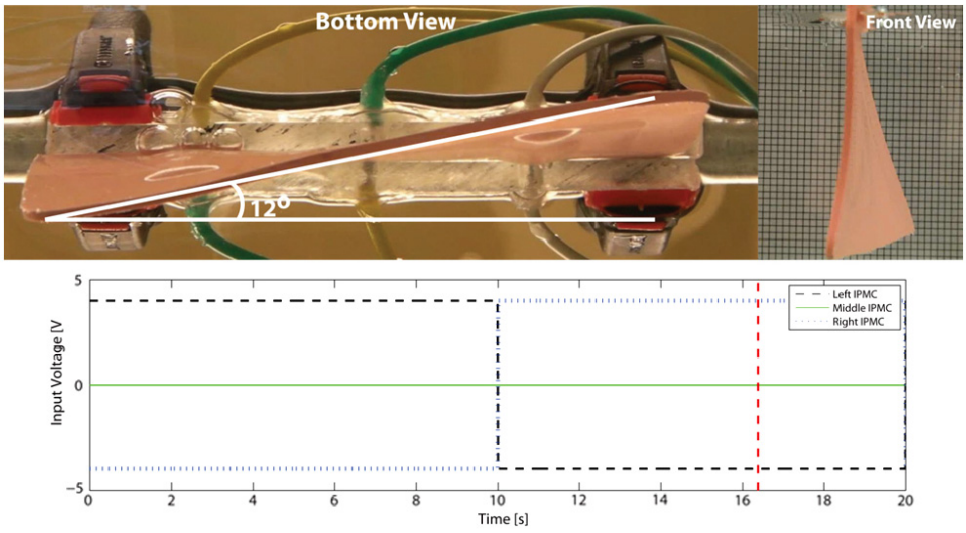

Figure 11. Two views depicting the maximum twist angle achieved for FIN-A with 4 V square wave input. Bottom: the input signal and the time of maximum deflection noted by the red dotted line.

for conducting the test. The system is shown in figure 12, and it consists of a computer and data acquisition system, a 100-gallon water tank, and a motorized platform (with force transducer) for moving the fin through the water at a prescribed speed. Figure 13 shows the FIN-C mounted during a routine test.

Two IPMC strip actuators were embedded into the FIN-B design as shown in figure 13. The governing equations for the lift and drag forces are given by

$$F_l = \tfrac{1}{2} C_l A_l \rho v^2, \tag{3}$$

$$F_d = \tfrac{1}{2} C_d A_d \rho v^2, \tag{4}$$

where C_l and C_d are the lift and drag coefficients, respectively; A_l and A_d are the area of the orthographic projection of the fin—on a plane perpendicular to the direction of motion; ρ is the density of the fluid; and v is the velocity of the fin relative to the fluid. In the experiments, the velocity was chosen as $v = 21$ cm s^{-1}.

The effects on the lift and drag forces when the IPMC actuators are driven by 3, 6, and 8 V are shown in figure 14. The input voltage is proportional to the twist angle of the fin. As shown in figure 14(a), the maximum increase in drag on the fin was approximately 18%. Likewise, the lift was significantly affected, with a maximum increase of 450%. The measured lift-to-drag ratio is approximately 6.7. Using equations (3) and (4) and the measured lift and drag forces, the plot of the drag effects ($C_d A_d$) versus the lift effects ($C_l A_l$) is shown in figure 14(b).

In summary, the results of the performance of the two prototype IPMC-based fin structures demonstrate that IPMCs can be embedded into a soft boot structure to create

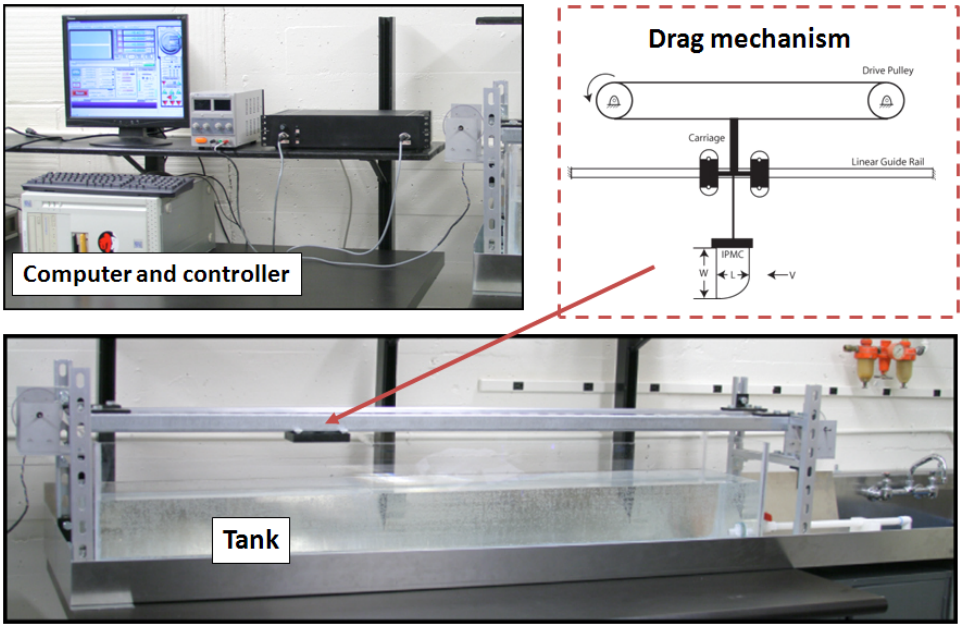

Figure 12. Drag tank experiment which consists of a computer and data acquisition system, a 100-gallon water tank, and a motorized platform (with force transducer) for moving the fin through the water at a prescribed speed.

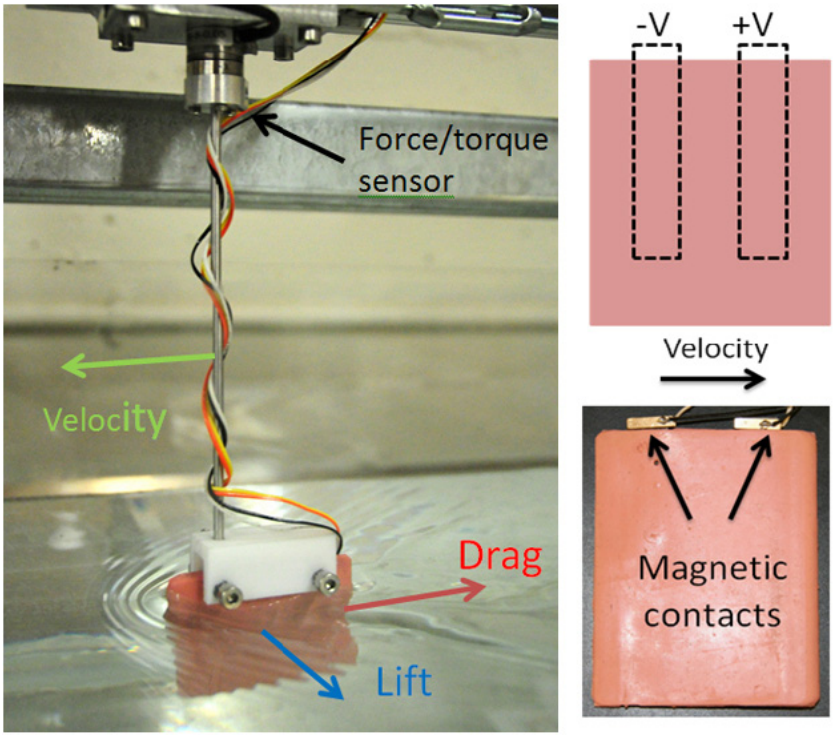

Figure 13. Experimental setup to measure lift and drag forces on boot-IPMC fin (FIN-B) in the drag tank.

deformable control surfaces capable of bending and twisting motion. As indicated by the drag tank test results, the lift and drag characteristics of the IPMC-based fins can be actively controlled for applications such as active propeller blades or control surfaces on underwater vehicles. One of the main advantages of embedding the IPMC within a soft boot structure is the reduction of the manufacturing costs since a small number of individual standard IPMC strip actuators are needed to create both bending and twisting motion.

5. Conclusions

This paper explored the approach to embed IPMC strip actuators into a soft boot structure to create an active

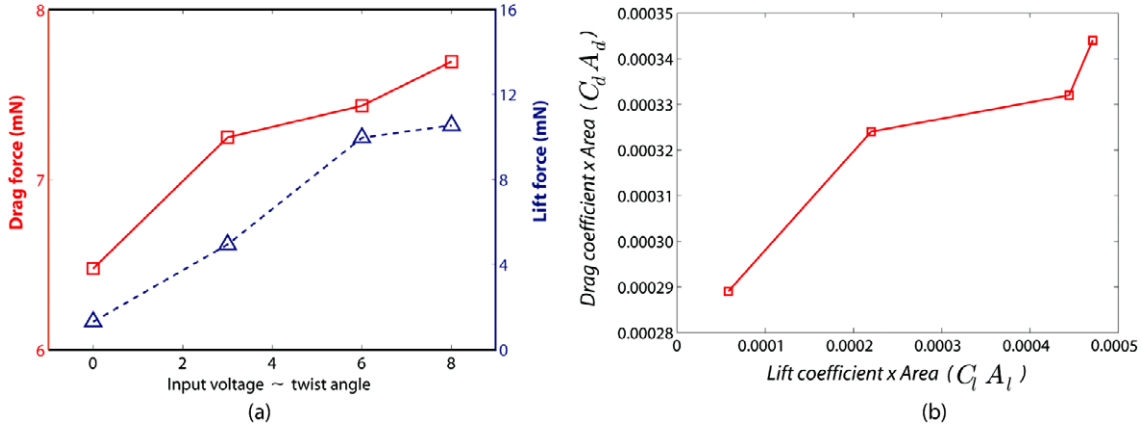

Figure 14. (a) Lift and drag forces versus fin angle of twist. (b) Drag effects versus lift effects.

bio-inspired fin capable of bending and twisting motion. For the 90 mm wide × 60 mm long × 1.5 mm thick prototype fin, the measured maximum tip displacement was approximately 44 mm and the twist angle of the fin exceeded 10°. Lift and drag measurements in water where the prototype fin with an airfoil profile was dragged at a velocity of 21 cm s^{-1} showed that the lift and drag forces can be affected by controlling the IPMCs embedded into the fin structure. These results suggest that such active fin designs can be used for developing active propeller blades or control surfaces on underwater vehicles.

Acknowledgments

Authors gratefully acknowledge support from the Office of Naval Research, grant number N000140910218, and collaboration with P Bandyopadhyay at the Naval Undersea Warfare Center (NUWC), Rhode Island.

References

[1] Kim K J, Yim W, Paquette J W and Kim D 2007 Ionic polymer–metal composites for underwater operation *J. Intell. Mater. Syst. Struct.* **18** 123–31

[2] Yamakita M, Sera A, Kamamichi N, Asaka K and Luo Z-W, Integrated design of IPMC actuator/sensor *IEEE Int. Conf. on Robotics and Automation* pp 1834–9

[3] Yim W, Lee J and Kim K J 2007 An artificial muscle actuator for biomimetic underwater propulsors *Bioinspir. Biomim.* **2** S31–41

[4] Chen Z, Shatara S and Tan X 2010 Modeling of biomimetic robotic fish propelled by an ionic polymer–metal composite caudal fin *IEEE/ASME Trans. Mechatron.* **15** 448–59

[5] Aureli M, Kopman V and Porfiri M 2010 Free-locomotion of underwater vehicles actuated by ionic polymer metal composites *IEEE/ASME Trans. Mechatron.* **15** 603–14

[6] Biddiss E and Chau T 2006 Electroactive polymeric sensors in hand prostheses: bending response of an ionic polymer metal composite *Med. Eng. Phys.* **28** 568–78

[7] Yoon W J, Reinhall P G and Seibel E J 2007 Analysis of electro-active polymer bending: a component in a low cost ultrathin scanning endoscope *Sensors Actuators* A **133** 506–17

[8] Chen Z, Shen Y, Xi N and Tan X 2007 Integrated sensing for ionic polymer–metal composite actuators using PVDF thin films *Smart Mater. Struct.* **16** S262–71

[9] Lee M J, Jung S H, Lee S, Mun M S and Moon I 2006 Control of IPMC-based artificial muscle for myoelectric hand prosthesis *The First IEEE/RAS-EMBS Int. Conf. on Biomedical Robotics and Biomechatronics* pp 1172–7

[10] Brufau-Penella J, Puig-Vidal M, Giannone P, Graziani S and Strazzeri S 2008 Characterization of the harvesting capabilities of an ionic polymer metal composite device *Smart Mater. Struct.* **17** 015009

[11] Tiwari R, Kim K J and Kim S 2008 Ionic polymer–metal composite as energy harvesters *Smart Struct. Syst.* **4** 549–63

[12] Aureli M, Prince C, Porfiri M and Peterson S D 2010 Energy harvesting from base excitation of ionic polymer metal composites in fluid environments *Smart Mater. Struct.* **19** 015003

[13] Yeom S W and Oh I K 2008 Fabrication and evaluation of biomimetic jellyfish robot using IPMC *Adv. Sci. Technol.* **58** 171–6

[14] Lauder G V 2007 How fish swim: flexible fin thrusters as an EAP platform *(EAPAD): SPIE Smart Structures and Materials: Electroactive Polymer Actuators and Devices* vol 6524 p 652402

[15] Kim B, Kim D-H, Jung J J and Park J-O 2005 A biomimetic undulatory tadpole robot using ionic polymer–metal composite actuators *Smart Mater. Struct.* **14** 1579–85

[16] Hubbard J, Fleming M, Leang K K, Palmre V, Pugal D and Kim K J 2011 Characterization of sectored-electrode iPMC-based propulsors for underwater locomotion *(SMASIS): ASME Conf. on Smart Materials, Adaptive Structures and Intelligent Systems*

[17] Jeon J H, Yeom S-W and Oh I-K 2008 Fabrication and actuation of ionic polymer metal composites patterned by combining electroplating with electroless plating *Composites* A **39** 588–96

[18] Kim K J, Pugal D and Leang K K 2011 A twistable ionic polymer–metal composite artificial muscle for marine applications *Mar. Technol. Soc. J.* **45** 83–98

[19] Kruusamae K, Brunetto P, Graziani S, Punning A, Di Pasquale G and Aabloo A 2009 Self-sensing ionic polymer–metal composite actuating device with patterned surface electrodes *Polym. Int.* **59** 300–4

[20] Punning A, Anton M, Kruusmaa M and Aabloo A 2005 An engineering approach to reduced power consumption of IPMC (ion-polymer metal composite) actuators *(ICRA): Int. Conf. on Robotics* pp 856–63

[21] Kruusmaa M, Hunt A, Punning A, Anton M and Aabloo A 2008 A linked manipulator with ion-polymer metal composite (IPMC) joints for soft- and micromanipulation *(ICRA): IEEE Int. Conf. on Robotics and Automation* pp 3588–93

[22] Arena P, Bonomo C, Fortuna L, Frasca M and Graziani S 2006 Design and control of an IPMC wormlike robot *IEEE Trans. Syst. Man Cybern.* B **36** 1044–52
[23] Kamamichi N, Yamakita M, Asaka K and Luo Z-W, A snake-like swimming robot using IPMC actuator/sensor *IEEE Int. Conf. on Robotics and Automation* pp 1812–7
[24] Tiwari R and Kim K J 2010 Disc-shaped ionic polymer metal composites for use in mechano-electrical applications *Smart Mater. Struct.* **19** 065016
[25] Li S-L, Kim W-Y, Cheng T H and Oh I-K 2011 A helical ionic polymer–metal composite actuator for radius control of biomedical active stents *Smart Mater. Struct.* **20** 035008
[26] Kim S J, Pugal D, Wong J, Kim K J and Yim W, A bio-inspired multi degree of freedom actuator based on a novel cylindrical ionic polymer–metal composite material *15th Int. Conf. on Advanced Robotics*
[27] Kim K J and Shahinpoor M 2003 Ionic polymer–metal composites: II. Manufacturing techniques *Smart Mater. Struct.* **12** 65–79
[28] Akle B J, Leo D J, Hickner M A and McGrath J E 2005 Correlation of capacitance and actuation in ionomeric polymer transducers *J. Mater. Sci.* **40** 3715–24
[29] Aureli M, Lin W and Porfiri M 2009 On the capacitance-boost of ionic polymer metal composites due to electroless plating: theory and experiments *J. Appl. Phys.* **105** 104911
[30] Nam J D, Choi H R, Tak Y S and Kim K J 2003 Novel electroactive, silicate nanocomposites prepared to be used as actuators and artificial muscles *Sensors Actuators* A **105** 83–90
[31] Nguyen V K, Lee J W and Yoo Y 2007 Characteristics and performance of ionic polymer–metal composite actuators based on Nafion/layered silicate and Nafion/silica nanocomposites *Sensors Actuators* B **120** 529–37
[32] Shahinpoor M and Kim K J 2001 Ionic polymer–metal composites: I. Fundamentals *Smart Mater. Struct.* **10** 819–33
[33] Kim K J and Shahinpoor M 2002 A novel method of manufacturing three-dimensional ionic polymer–metal composites (IPMCS) biomimetic sensors, actuators and artificial muscles *Polymer* **43** 797–802
[34] Kim B, Kim B M, Ryu J, Oh I-H, Lee S-K, Cha S-E and Pak J 2003 Analysis of mechanical characteristics of the ionic polymer metal composite (IPMC) actuator using cast ion-exchange film *(EAPAD): SPIE Smart Structures and Materials: Electroactive Polymer Actuators and Devices* vol 5051 pp 486–95
[35] Pak J J, Kim J, Oh S W, Son J H, Cho S H, Lee S-K, Park J-Y and Kim B, Fabrication of ionic-polymer–metal-composite (IPMC) micropump using a commercial nafion *SPIE Smart Structures and Materials: Electroactive Polymer Actuators and Devices (EAPAD)* vol 5385 pp 272–80
[36] Shan Y and Leang K K 2009 Frequency-weighted feedforward control for dynamic compensation in ionic polymer–metal composite actuators *Smart Mater. Struct.* **18** 125016
[37] Lee S J, Han M J, Kim S J, Jho J Y, Lee H Y and Kim Y H 2006 A new fabrication method for IPMC actuators and application to artificial fingers *Smart Mater. Struct.* **15** 1217–24
[38] Menozzi A, Leinhos H A, Beal D N and Bandyopadhyay P R 2008 Open-loop control of a multifin biorobotic rigid underwater vehicle *IEEE J. Ocean. Eng.* **33** 59–68
[39] Leang K K, Shan Y, Song S and Kim K J 2012 Integrated sensing for IPMC actuators using strain gages for underwater applications *IEEE/ASME Trans. Mechatronics* **17** 345–55